

## Effect of Applied of Pre-Stresses on Corrosion Behavior of 304 Stainless Steel in 1N H<sub>2</sub>SO<sub>4</sub>

**Dr. Sami Ibrahim Jafar**

Production & Metallurgy Engineering Department/ University Of Technological /Baghdad

**Dr. Israa Abud Alkadir**

Production & Metallurgy Engineering Department/ University Of Technological /Baghdad

**Samah Abdul Kareem Khashin**

Production & Metallurgy Engineering Department/ University Of Technological /Baghdad

Email:samahkareem@yahoo.com

Received on:6/7/2015 & Accepted on:17/12/2015

### ABSTRACT

This research is devoted to study the effect of applying different pre-tensile stresses (255,305,355,405,455,505 555 and 605) MPa on the microstructure, hardness and corrosion behavior of 304 stainless steel in 1N H<sub>2</sub>SO<sub>4</sub>. The stress-strain curve was drawn for standard (304) stainless steel in laboratory environment. The curve was divided into three zones. At zone one the values of elastic pre-stresses vary between ( $\sigma_0 - \sigma_{pro.}$ ) MPa. The results showed; that the corrosion rate was very little increased compared with that of as received (304) stainless steel. The microstructure presented undeformed austenitic grains and the hardness value was (157.433) Hv. At zone two the value of plastic pre-stress varies between ( $\sigma_{pro.} - \sigma_{U.T.S}$ ) MPa. The corrosion rate increases after applying pre-stress between ( $\sigma_{255} - \sigma_{455}$ ) MPa. The microstructure showed that the austenitic grains begin to deform in the direction of applied pre-stresses. The maximum hardness at this region was (229.2) Hv, but at higher pre-stress ( $\sigma_{455} - \sigma_{605}$ ) MPa, the corrosion rate decreases. The microstructure inspection shows the deformed austenitic grain and  $\alpha$ -martensitic phase needle are appeared inside austenitic grains and the hardness reached the maximum value (332.433) Hv. At zone three the values of pre-stresses are between ( $\sigma_{605} - \sigma_f$ ) MPa. The results showed that the corrosion rate increases. The investigation of microstructure showed that there are distortion in austenitic grains and  $\alpha$ - martensite phase observed inside austenitic grains. The hardness reached the maximum value at (354.3) Hv. The necking of gauge length of specimens occurs in specimens and this leads to deterioration in original properties

**Keywords:** Stainless steel, Corrosion resistance, Mechanical properties.

تأثير تسليط الأجهادات المسبقة على سلوك تآكل الفولاذ المقاوم للصدأ نوع 304 في محلول N H<sub>2</sub>SO<sub>4</sub>

الخلاصة

يهدف البحث الحالي الى دراسة تأثير التشوه على البارد من خلال تسليط اجهادات شديدة مسبقة مختلفة القيم (255,305,355,405,455,505 555,605) ميكاباسكال على البنية المجهرية والصلادة المجهرية وسلوك التآكل للفولاذ المقاوم للصدأ نوع 304 في محلول 1N H<sub>2</sub>SO<sub>4</sub>. تم رسم منحني الاجهاد- الانفعال لعينة قياسية من 304 فولاذ مقاوم للصدأ في جو المختبر. قسم المنحني الى ثلاثة مناطق: المنطقة الاولى : تكون قيم الاجهادات المرن بين ( $\sigma_0 - \sigma_{pro}$ ) ميكاباسكال ، حيث أظهرت النتائج حدوث زيادة طفيفة في معدل التآكل مقارنة مع عينات غير مجهدة من الفولاذ المقاوم للصدأ 304 . وعند اجراء الفحص المجهرى تبين ان البنية الدقيقة هي عبارة عن حبيبات اوستنايتية غير مشوهة ومن نتائج فحص الصلادة كانت صلادة الفولاذ المقاومة للصدأ غير المجهد هي

(157.433Hv) وعند المنطقة الثانية: تتغير قيم الاجهاد اللدن المسبق بين ( $\sigma_{pro.} - \sigma_{U.T.S}$ ) ميكا باسكال، حيث أظهرت نتائج قياس معدل التآكل أن معدل التآكل قد ازداد بعد تسليط اجهاد المسبق بين ( $\sigma_{255} - \sigma_{405}$ ) ميكا باسكال . ومن نتائج فحص البنية المجهرية تبين ان البنية المجهرية هي عبارة حبيبات اوستنايتية مشوهة باتجاه الاجهاد المسلط وتبين من نتائج فحص الصلادة ان أعلى قيمة للصلادة في تلك المنطقة هي (229.2 Hv) لكن عند قيم الاجهادات المسبقة العالية بين ( $\sigma_{455} - \sigma_{605}$ ) ميكا باسكال ، انخفض معدل التآكل بشكل كبير. كما تبين من فحص البنية المجهرية انها عبارة عن حبيبات اوستنايتية مشوهة مع ظهور طور  $\alpha$ -martensitic أبري الشكل داخل حبيبات الاوستنايت، مما أدى ذلك الى ازدياد قيمة الصلادة حيث بلغت أعلى قيمة مقدارها (332.433 Hv) أما في المنطقة الثالثة : تتغير فيها قيم الاجهادات المسبقة المسلطة بين ( $\sigma_{605} - \sigma_f$ ) ميكا باسكال ، حيث أظهرت النتائج حدوث زيادة في معدل التآكل . ومن نتائج الفحص المجهرية تبين حدوث تشويه كبير لحبيبات الاوستنايت مقارنة بالاجهادات المسبقة المسلطة أعلاه إضافة الى وجود طور  $\alpha$ -martensitic أبري الشكل داخل حبيبات الاوستنايت ونسبته عالية ، حيث بلغت أفضل قيمة للصلادة (354.3 Hv) لكن التخصر الحاصل في العينات أدى الى حدوث تدهور الخواص الاصلية.

## INTRODUCTION

**T**ype 304 stainless steel offers excellent combinations of high strength, toughness and mechanical properties with high corrosion resistance.

These steels exhibit excellent resistance to a wide range of atmospheric, chemical, textile, petroleum and food industry exposures [1]. These Properties decide about their wide application in the chemical, machinery, food, automotive, nuclear and shipbuilding industries.

This type of steel has been employed in many applications ranging from pharmaceutical equipment to piping in the nuclear reactors.

Several researchers [2-5] studied the effect of the deformation on mechanical properties and corrosion resistance for many types of stainless steel and other alloys by using different techniques. **Peguet, et al [2]** studied the effect of rolling and tensile distortion on the pitting corrosion resistance of AISI 304 and AISI 430 stainless steels.

They concluded that the pitting corrosion had differently depending on down loading. The pit inception frequency shows a max. after 20% rolling lowering or 10% tensile distortion. The pit propagation rate increases progressively with rolling reduction, and pit re-passivation faculty reduced driving to a higher number of more regular pits, and the highest pit dissolve average is occurred for 20% cold-rolling. The repassivation ability decrease when the cold-working percentages rate increases, driving to a more macroscopically pit density. **Jin-long and Luo Hong-yun [3]** Studied the percentage of pre-strain (0%, 10%, 20%, 30%, 40%) of AISI 304 stainless steel and sensitization at 575°C by the binary loop electrochemical potentiokinetic reactivation process and scanning electron microscopes. The results for sensitized specimens show that the degree of sensitization effects on the electrochemical behavior and the resistance of corrosion of the passive layer. More reactivation current density occurs at 10% pre-strain, when compared with other sensitized specimens with 30% and 40% pre-strain. They concluded that the different chromium depleted zones leads change in compositions and thickness in passive film with more strains. **Ghosh et al [4]** studied the effects of cold deformation at varying amount of (10 %, 20%, 30%, 40%) at 0 °C on the microstructure and mechanical properties of an austenitic stainless steel. They concluded that at cold deformed (30% - 40%), the samples reveal the presence of  $\alpha$  martensite, while the non-deformed specimen showed only the austenitic microstructure. They concluded that deformation led to enhancement in hardness, yield strength and tensile strength values while the percent elongation was dropped. **Jingqiang Yang, et al [5]** studied the resistance of corrosion of DSS, type SAF2205 , SAF2507 in 3.5% NaCl and 2 mol/L HCl solution under different applied stresses 100 MPa, 300 MPa, 500 MPa and the percentage of pre-strain (5%, 10%, 15%). The corrosion resistance of 2205 DSS show a little decreases with increasing of elastic stress range. With increasing pre-strained level, they show that the pitting is allows present at located sites in austenite grains when the percentage of

pre-strain is lower than 5%. This is due to vary elastic stress range. The pitting was observed at intersection between ferrite and austenite grain boundaries. When pre-strain level is above 5% they observed that the elastic stress and strain rate had no effects on pitting corrosion but reduced the general corrosion resistance and the strain may be increase the instability of passive film, which accelerated the dissolution of passive layer.

The aim and the scope of this work is to determine the effect of applied pre-stresses at different values of (255,305,355,405,455,505,555,605)MPa on the microstructure, hardness and corrosion behaviors of 304 stainless steel in 1N H<sub>2</sub>SO<sub>4</sub>.

### Experimental Work

Table (1) lists the chemical composition of the as-received AISI304 stainless steel. Figure (1) shows the standard tensile test specimen, which used in this work according to ASTM E8M.

The tensile test was carried out at room temperature by applying a tensile load to obtained stress-strain curve as shown in Figure (2). The stress-strain curve divided into the following groups and an increase of 50 MPa after the value of yield stress ( $\sigma_{pro}$ ). The tensile test was conducted using a standard 2000KN capacity by using tensile machine, typeWDW-200E model in Production Engineering and Metallurgy Department, University of Technology.

### Corrosion test

The electrochemical behavior and corrosion test are done on the specimens as received and for specimens after pre-stresses (255,305,355,405,455,505,555,605, fracture stress) MPa. The corrosion tests were measured by Tafel Extrapolations Technique. The samples were exposed to 1N H<sub>2</sub>SO<sub>4</sub> solution. The electrochemical measurement was done at the Ministry of Science and Technology- Baghdad by using computerized potentate type PARSTAT 2273 / Advanced Measurement Technology, Inc. The electrochemical cell consists of working, electrode and reference electrodes. The reference electrode is a standard hydrogen electrode (S.H.E) bridged by a Laggin-Haber probe. The distance between the standard electrode and the surface of the specimen was set at about the optimum value of 1 mm.

### Microstructure, X-ray diffraction and Microhardness examination:

The microstructure test was examined by optical microscope using Metallographic microscope (MTM-1A, Japan). The phases present in stainless steel before and after pre-stressing were examined by using X-ray diffraction instrument type (XRD-7000 X-Ray diffractometer), model (maxima-x). While The microhardness test of the specimens was conducted using Digital Micro Vickers Hardness tester model TH 714.

### Results and discussion

Figures (3) to (12) represent the polarization curves of stainless steel 304 in 1N H<sub>2</sub>SO<sub>4</sub> solution before and after pre-stresses.

Figure (3) represents the potentiostatic curves of anodic and cathodic polarization of 304 Stainless steel in 1N H<sub>2</sub>SO<sub>4</sub> solution. The open circuit potential was (-375 mV) (S.H.E). The polarization curve started from this potential and passivation range started at (50 mV) in noble direction. The polarization curves were plotted at (10mVs<sup>-1</sup>) scanning rate. The potential range for the passivation region started at (50 - 1065) mV as shown in Table (2). The results represent to not change the value of the ( $E_{corr}$ ,  $I_{corr}$ , and  $E_{pit}$ ) for specimens as received when compared with elastic pre-stresses specimens can be due that the specimen returns to the original dimensions[6]. Figure [13,(a,b)] shows that the microstructure only one phase ( $\gamma$ ) grain with twinning has F.C.C crystal structure. Also the X-Ray diffraction analysis represent only ( $\gamma$ ) phase as shown in Figure [14, zone (I)].

Figure(4) shows the polarization curve of 304 stainless steel after exposing the specimen to elastic stress in 1 N H<sub>2</sub>SO<sub>4</sub>. It can be seen from the figure that there are some variations in

the values of electrochemical parameters between the polarization curve of as received Figure(3) and polarization curve of 304 stainless steel at a proof stress (255MPa) as shown in figure(4). This variation includes ( $I_{corr}$ ,  $I_{passive}$ ,  $i_{pit}$ ). The values of these parameters are of small order increase than of as nonstressed specimen. These results can be attributed to the non-differences in microstructures. The microstructure obtained, consists of one phase ( $\gamma$ ) grain. The specimen at offset stress region has higher corrosion rate than that of as non-stressed specimens. The passivation region of 304 stainless steel after elastic deformation is not irregular as shown in Figure (3) and the starting and finishing of the passivation have the same values.  $E_{pit}$  (1062mV) and  $I_{pit}$  ( $4.2 \times 10^{-1} \mu A/cm^2$ ) as shown in Table (2).

Corrosion resistance test of 304 stainless steel was carried out after pre-plastic applied stress with values (305,355,405,455,505,555,605) MPa in 1N H<sub>2</sub>SO<sub>4</sub>. Potentiostatic polarization curves are illustrated in Figures (5) to (11). These figures revealed that corrosion resistance of 304 stainless steel affected by plastic deformation. The corrosion resistance decreases with increasing of pre-plastic stress level and noticeably with increasing pre-stresses due to some changes including structure and distribution of dislocations Figure (13). The dislocation density increases and the stacking fault density increased with the increasing the value of pre-stress, the ( $\gamma$ ) grains are also deformed and elongated due to pre-stress deformation as shown in Figure [13,(c,d)]. The stability of passive film decreases and the corrosion rate increases also. This clearly shown in Figure [14, zone (II)], it represents that the pitting in this case is more than that in case (as received) specimens. It was observed that, the passive film was formed in pre-stress specimens more easily than that of unstressed specimens. At ( $\sigma = 605$ ) MPa, the corrosion resistance decreases in 304 stainless steel in 1N H<sub>2</sub>SO<sub>4</sub> due to causing voids at the matrix-inclusion interface. Figures (4, 5, 6, 7) show polarization curves of (304) stainless steel after pre-plastic stresses. The stainless steel shows active-passive behavior. It is clear that after pre-stress ( $\sigma = 605$ ) MPa, corrosion resistance and passive range of ( $2.1 \times 10^{-1}$ -  $2.3 \times 10^{-2}$ ) decrease, according to Figures (3,4,5,6,7,8,9,10,11,12), the pre-plastic stress has a significant influence on polarization curves. Generally, high plastic tensile stress decreases corrosion resistance of stainless steel due to change in the nature of surface and change in the nature of passive film. This means, that pre-plastic stress can also change the properties of the passive film in 304 stainless steel, the stability of the passive film depends up the values of plastic pre-stress deformation. When the plastic deformation increases from 75.2% to U.T.S., higher deformation occurs. This is related to the value of plastic deformation (455-605) MPa which induces phase transformation to ( $\alpha$ - martensite) phase, the needle shaped phase forms within austenitic grain as shown in Figure [13,(e)]. The X-Ray diffraction analysis also presents these two phase ( $\gamma + \alpha$ ) of martensite as shown in Figure [14,zone(III)]. The obstacles like grain boundary twinning boundary and ( $\gamma / \alpha$ ) marten site interface makes the dislocation movement very difficult and the strengthening mechanisms occurs [7]. Therefore the hardness increases as demonstrated in Figure [13, zone (III)]. This leads to increase corrosion resistance due to increase the stability of passive film on the surface of (304) stainless steel. This will lead to decrease the pitting formation as shown in Figure [13,(f)]. The cyclic polarization as shown in Figures (4-3, 4-6, 4-7, 4-8) illustrated that the width of hysteresis loop is increased as pre-stress increases. Figures (3,5,6,7) show the change in  $E_p$  and  $E_{pit}$ . It is seen that these critical potentials are lower than those of unstressed condition. The results indicate that pitting potential is more active than that without stress. A comparison between the curves at different pre-stresses reveals that at higher pre-stress, the pitting current density was different with respect to low pre-stress conditions. The passive range in low pre-stress is increased with respect to U.T.S stress. Effect of plastic pre-stress on the development of pitting corrosion showed that the plastic pre-stress deformation plays an important role in acceleration formation of pitting corrosion. Work of [8] reported that the accumulation of dislocation close to grain boundaries area can result in high stress concentration which makes pitting corrosion happen easily on these sites. The results show a detrimental effect of deformation on the pitting

corrosion of stainless steel for deformations corresponding to pre-stress at U.T.S stress, whereas the localized corrosion resistance of the pre-stress 304 stainless steel over 75.2% increased comparatively to that without pre-stress. The decrease in pitting corrosion from  $\sigma_{42.14\%}$  (1 $\epsilon$ ) to  $\sigma_{75.2\%}$  (31.8  $\epsilon$ ) was correlated with the defects created in the passive film. The very high values of stress (more than 75.2%) on the other hand, resulted in blocking of the voids mainly at the interface between inclusions and the matrix. It can be concluded that corrosion resistance is decreased due to plastic deformation. The breakdown of Epit & Ep is evaluated by cyclic potentiostatic method in 1N H<sub>2</sub>SO<sub>4</sub>. The cyclic polarization in Figures (3,5,6,7) shows, width of hysteresis loop is increased as pre-stress increases.

It has been observed that the microstructure of the steel which deforms at a degree higher than  $\sigma_{U.T.S}$  as shown in Figure (12) will be elongated parallel toward the tensile direction and there are some dark areas in the structure referred to higher strain induced. Elongated austenitic grains are characterized by the deformed state of (304) stainless steel whereas the grains undergo elongation in the tensile direction. Perversely [9] showed that the plastic deformation in the cold working of the Fe-Cr-Ni steel increased with an increasing degree of deformation ( $\sigma_{U.T.S} - \sigma_f$ ).

The microstructure as shown in Figure [13,(i-j)], has two phases ( $\gamma + \alpha$ ) of martensite and the elongation of ( $\gamma$ ) grains increases with the directional of tensile stress and the internal stress and strain field increase. The dislocation density increases more than in the plastic zone (III). This leads to increase the hardness values to (332.433-354.3) Hv as represent in Figure [13, zone (IV)]. The X-Ray diffraction analysis demonstrates that there are two phases ( $\alpha$ ) martensite and ( $\gamma$ ) phases as shown in Figure (14). At the ultimate tensile strength, 304 stainless steel demonstrates that the value of the strain will be about (97.1%).

At the higher value of stress after the U.T.S to fracture show that after maximum load ( $\sigma_{U.T.S}$ ), the 304 stainless steel is characterized by the reduction in cross-section of area and the gauge length will be necking and then failure happens. It was found that this will be changing the structure and the dimension of gauge length. The corrosion current density is higher than that of corrosion current density for the non-stressed specimens. These results confirm that the corrosion resistance related to the changes in the microstructure. Table (2) shows the data of corrosion current density, current density of passivation and current density of initiation. When the stainless steel deform after U.T.S, useful value is very poor because the material loses its mechanical properties. The study on corrosion of the 304 stainless steel after pre-stresses below U.T.S confirms that the corrosion resistance of 304 stainless steel measured 1N H<sub>2</sub>SO<sub>4</sub> also decreases.

## CONCLUSIONS

The conclusions drawn from this study are:

- 1-The open circuit potential value of (304) stainless steel in 1N H<sub>2</sub>SO<sub>4</sub> is (-375 mV).
- 2-The passivation region started when the surface of specimen is coated with chromium and nickel oxides. The chromium oxide (Cr<sub>2</sub>O<sub>3</sub>) is the main component of the passive film. The passive potential started T 490 mV and finished at +1065mV.
- 3-The elastic region is extended to 255MPa (offset strength yield) and when the load is removed the specimen returns to its original dimension. The specimen of (304) stainless steel under elastic stresses has a small variation in corrosion behavior compared with corrosion behavior with unstressed condition.
- 4- After pre-plastic stresses between (255-405) MPa, some changes in structure and distribution of dislocation therefore the corrosion resistance decreases and the pitting corrosion was more than that of specimen under elastic pre-stresses.

5-Under pre-plastic stresses (455-605) MPa, two phases of ( $\gamma+\alpha$ ) are observed in microstructure and these phases lead to some improvement in corrosion resistance and to decrease in pitting corrosion.

6- When the pre-stresses reaches higher pre-stresses than  $\sigma_{U.T.S}$  (605) MPa, the specimens undergo elongation and get necked so that the cross sectional area would be smaller than that for non-stressed condition and corrosion resistance would be decreased.

7-The hardness increased with increasing pre-stresses.

**Table (1).Chemical composition of 304 stainless steel**

Element%	Standard%	Measured%
Carbon	0.08 max	0.07
Manganese	2.0	1.4
Phosphorus	0.045	-
Sulfur	0.03	-
Silicon	0.75	0.64
Chromium	18-20	18.5
Nickel	8-12	10.2
Molybdenum	0.38	0.30
Copper	0.12	0.10
Iron	Balance	Balance

**Table (2).Corrosion parameters of 304 stainless steel in 1N H<sub>2</sub>SO<sub>4</sub>.**

Conditions parameters	As $\sigma$ received	$\sigma_{255}$	$\sigma_{305}$	$\sigma_{355}$	$\sigma_{405}$	$\sigma_{455}$	$\sigma_{505}$	$\sigma_{555}$	$\sigma_{605}$	$\sigma_f$
E0	-375	-360	-420	-450	-450	-400	-401	-403	-405	-410
I0	$1 \cdot 10^{-2}$	$1.5 \cdot 10^{-2}$	$3 \cdot 10^{-1}$	$3.5 \cdot 10^{-2}$	$3 \cdot 10^{-2}$	$1.3 \cdot 10^{-2}$	$1.5 \cdot 10^{-2}$	$1.8 \cdot 10^{-2}$	$2 \cdot 10^{-2}$	$4 \cdot 10^{-1}$
Ecorr	-400	-400	-460	-460	-460	-400	-405	-408	-410	-460
Icorr	$2 \cdot 10^{-1}$	$2 \cdot 10^{-1}$	$3 \cdot 10^{-1}$	$3.5 \cdot 10^{-1}$	$4 \cdot 10^{-1}$	$1.5 \cdot 10^{-2}$	$1 \cdot 10^{-2}$	$0.8 \cdot 10^{-2}$	$0.5 \cdot 10^{-2}$	$3 \cdot 10^{-1}$
Epass	50	60	-120	-215	-220	-200	-190	-185	-175	-250
Ipass	$1.5 \cdot 10^{-2}$	$2.1 \cdot 10^{-1}$	$6 \cdot 10^{-1}$	$5.8 \cdot 10^{-1}$	$6 \cdot 10^{-1}$	$2.3 \cdot 10^{-2}$	$2.5 \cdot 10^{-2}$	$2.8 \cdot 10^{-2}$	$3 \cdot 10^{-2}$	$3.5 \cdot 10^{-1}$
Epit	1035	1040	1040	1030	1035	1042	1043	1045	1050	1020
Ipit	$4 \cdot 10^{-4}$	$4.2 \cdot 10^{-1}$	$3.5 \cdot 10^{-1}$	$1.5 \cdot 10^{-1}$	$4.3 \cdot 10^{-1}$	$2.5 \cdot 10^{-1}$	$3.5 \cdot 10^{-1}$	$2 \cdot 10^{-1}$	$3 \cdot 10^{-1}$	$5.5 \cdot 10^{-1}$
Etran	1065	1062	1063	1065	1062	1060	1050	1062	1060	1045
Itran	$8 \cdot 10^{-7}$	$7.5 \cdot 10^{-1}$	$3.5 \cdot 10^{-1}$	$3.8 \cdot 10^{-1}$	$4 \cdot 10^{-1}$	$8.5 \cdot 10^{-1}$	$9 \cdot 10^{-1}$	$3.5 \cdot 10^{-2}$	$3.8 \cdot 10^{-2}$	$3 \cdot 10^{-1}$

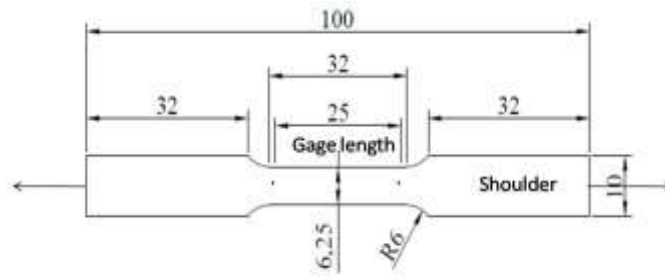


Figure. (1) The tensile specimen, showing:

- overall length=100mm.
- gage length=25mm.
- width=10mm.
- thickness=3mm.

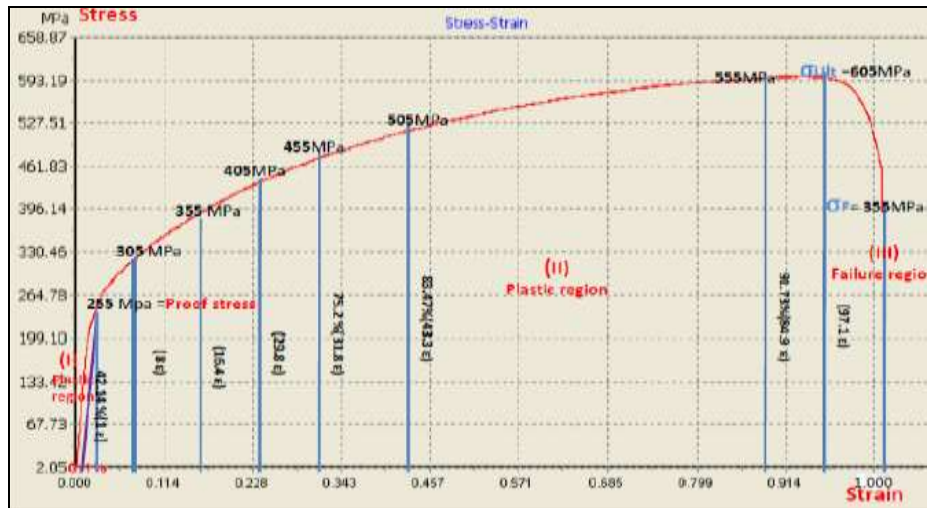


Figure.(2) Stress-strain curve of specimen as received.

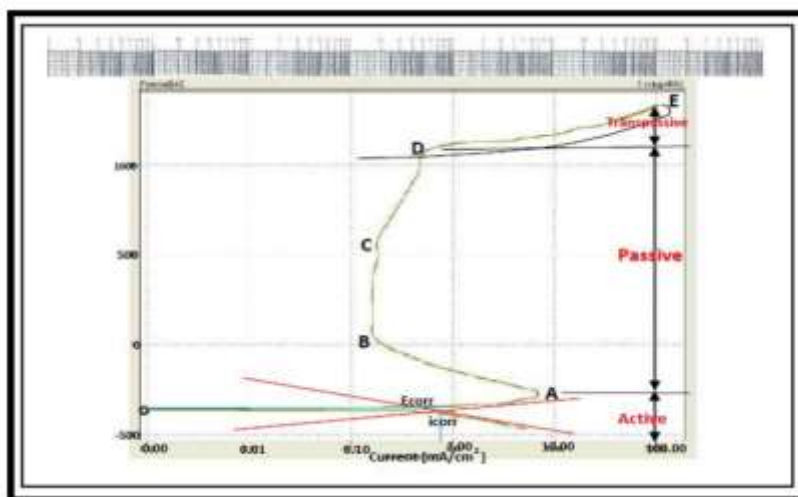


Figure.(3) Corrosion behavior of specimen as received.

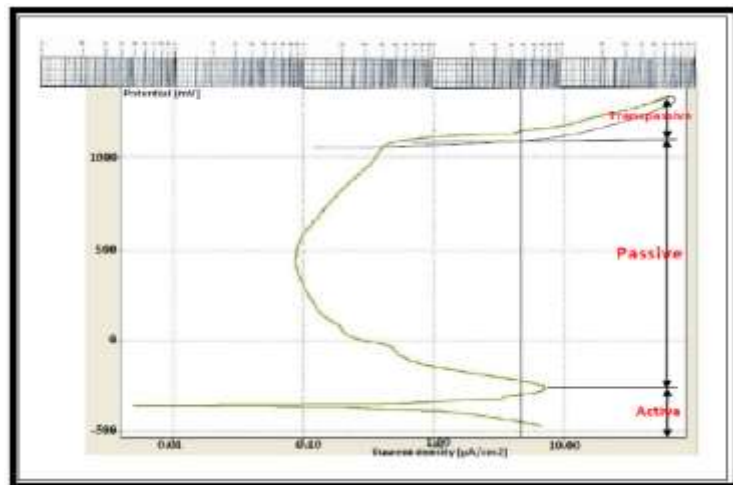


Figure. (4) Corrosion behavior of specimen in proof stress (255 MPa).

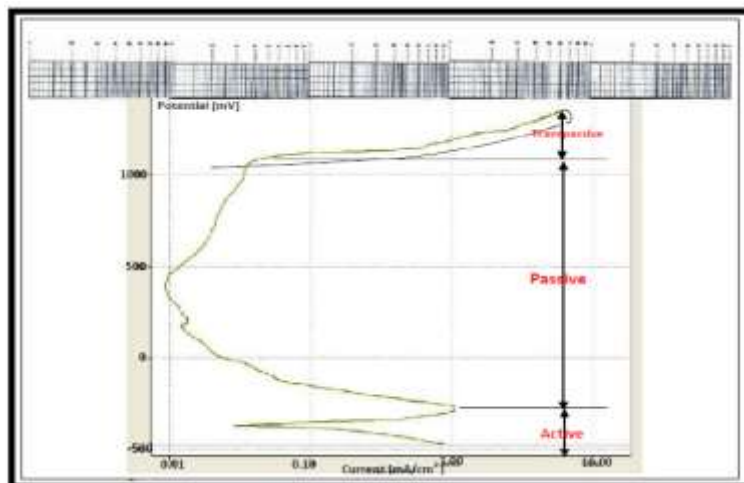


Figure. (5) Corrosion behavior of specimen at (305 MPa).

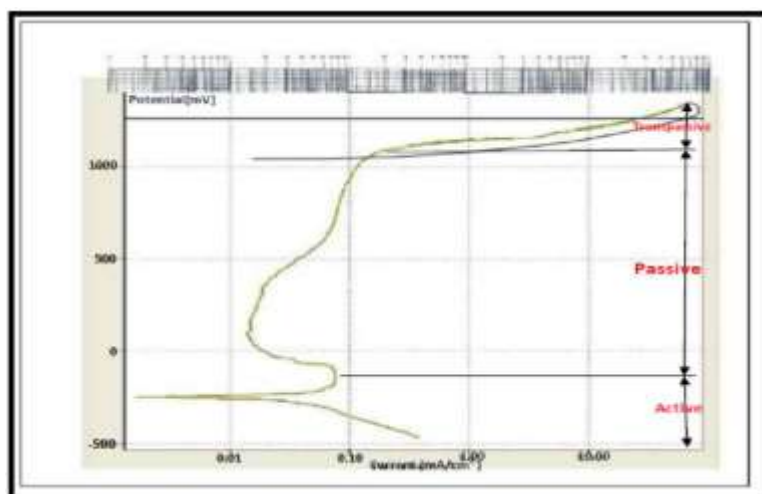


Figure. (6) Corrosion behavior of specimen at (355 MPa).

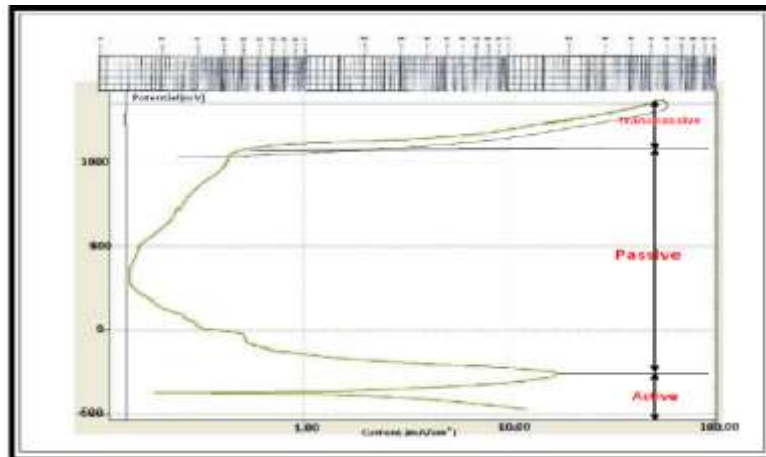


Figure. (7) Corrosion behavior of specimen at (405 MPa).

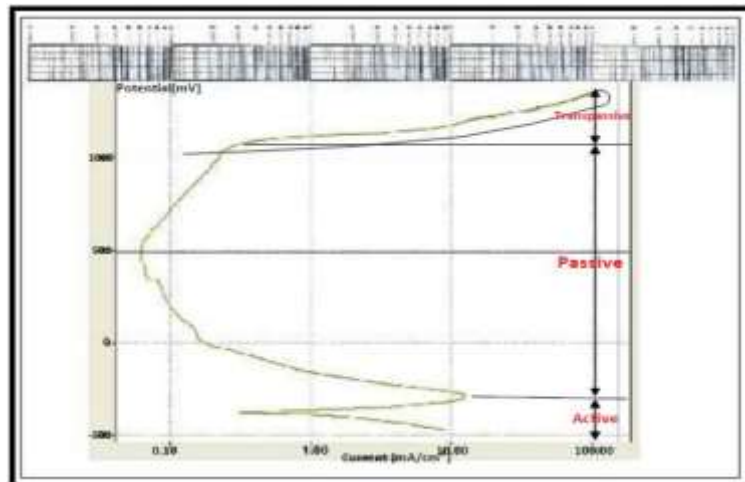


Figure.(8) Corrosion behavior of specimen at (455 MPa).

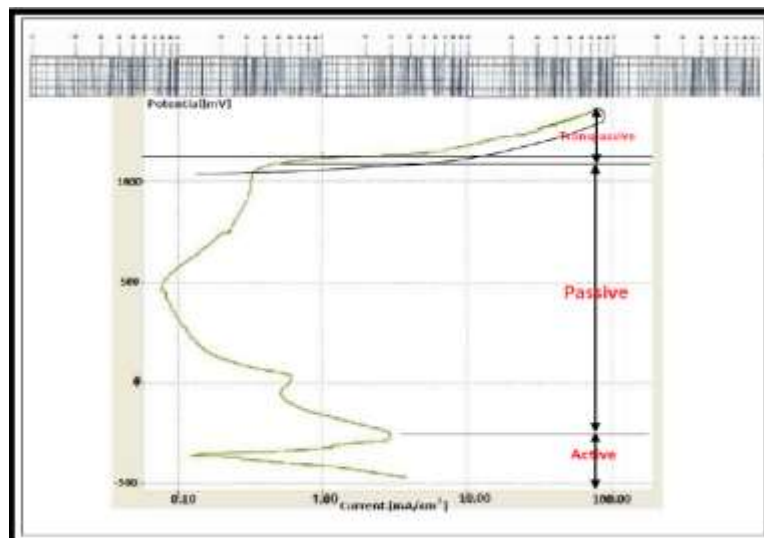


Figure. (9) Corrosion behavior of specimen at (505 MPa).

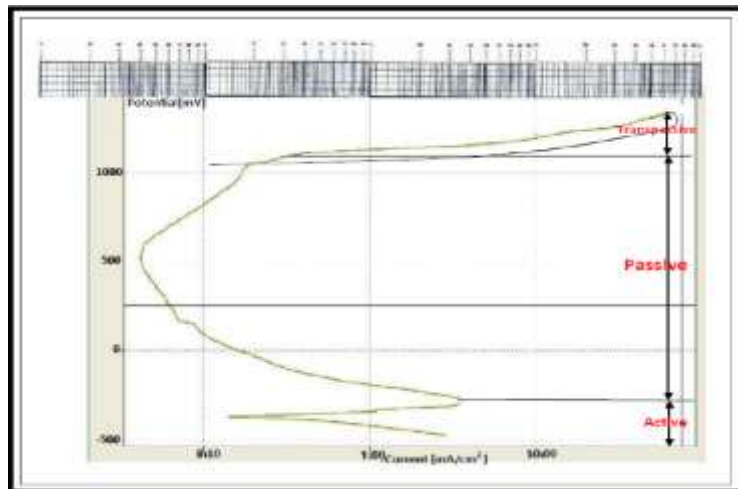


Figure. (10) Corrosion behavior of specimen at (555 MPa).

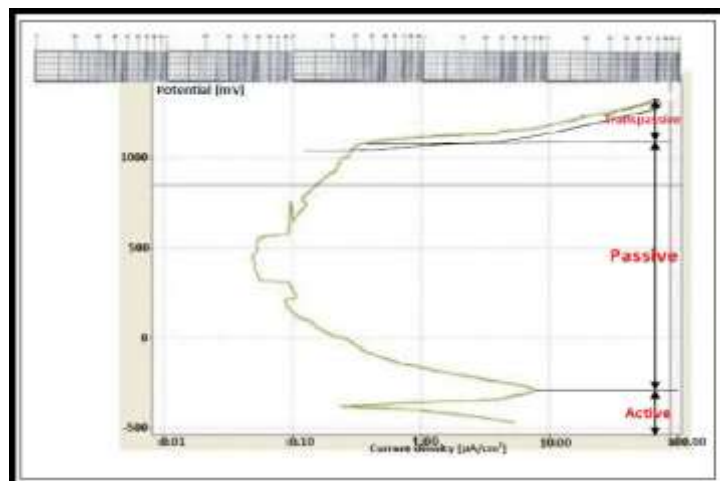


Figure. (11) Corrosion behavior of specimen at (605 MPa).

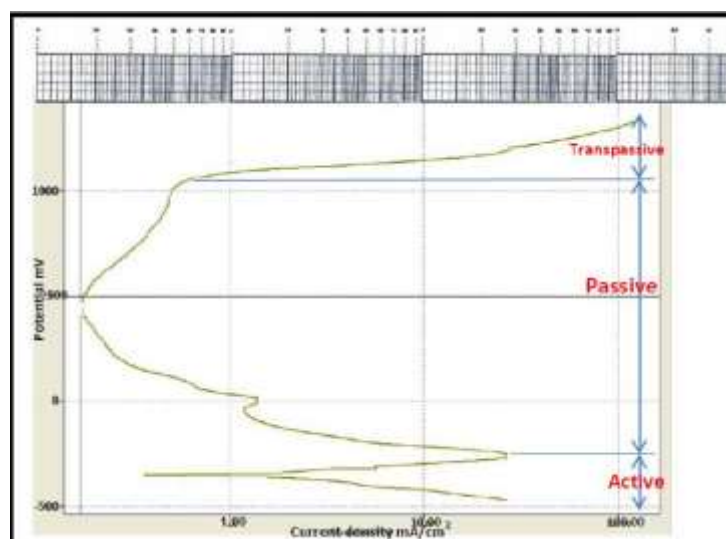


Figure.(12) Corrosion behavior of specimen at failure.

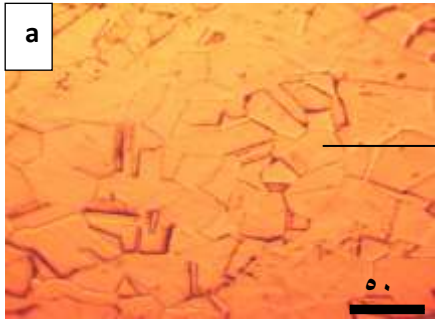
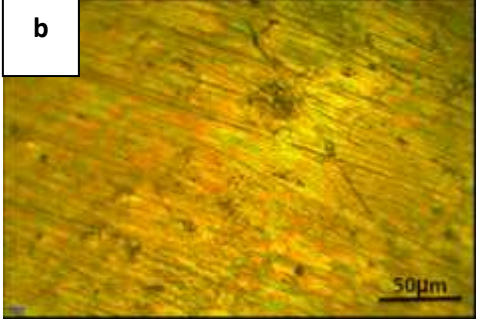
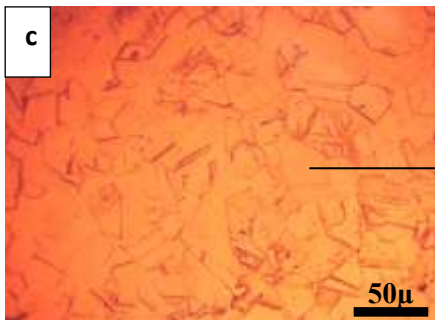
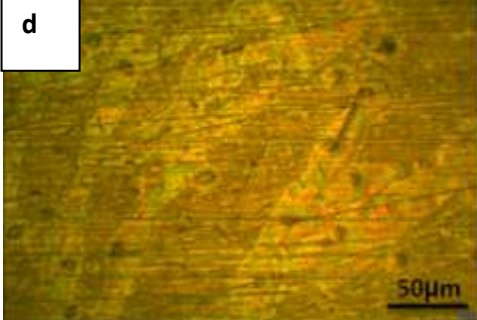
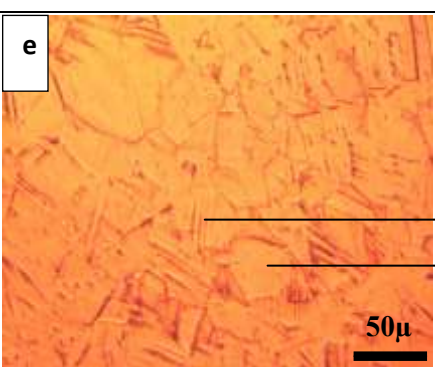
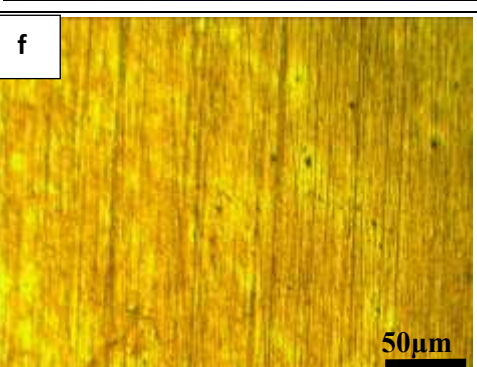
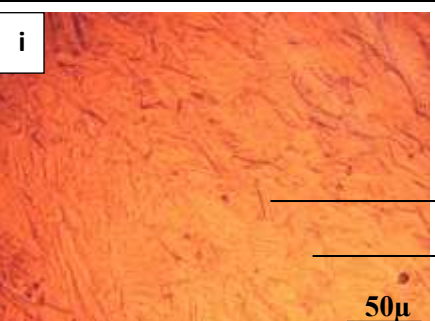
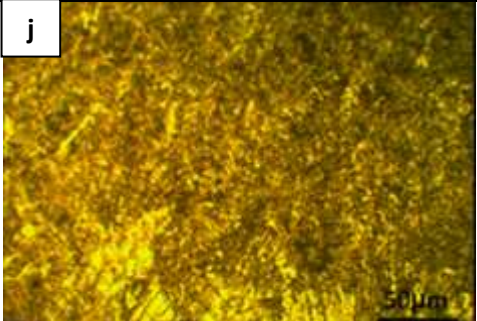
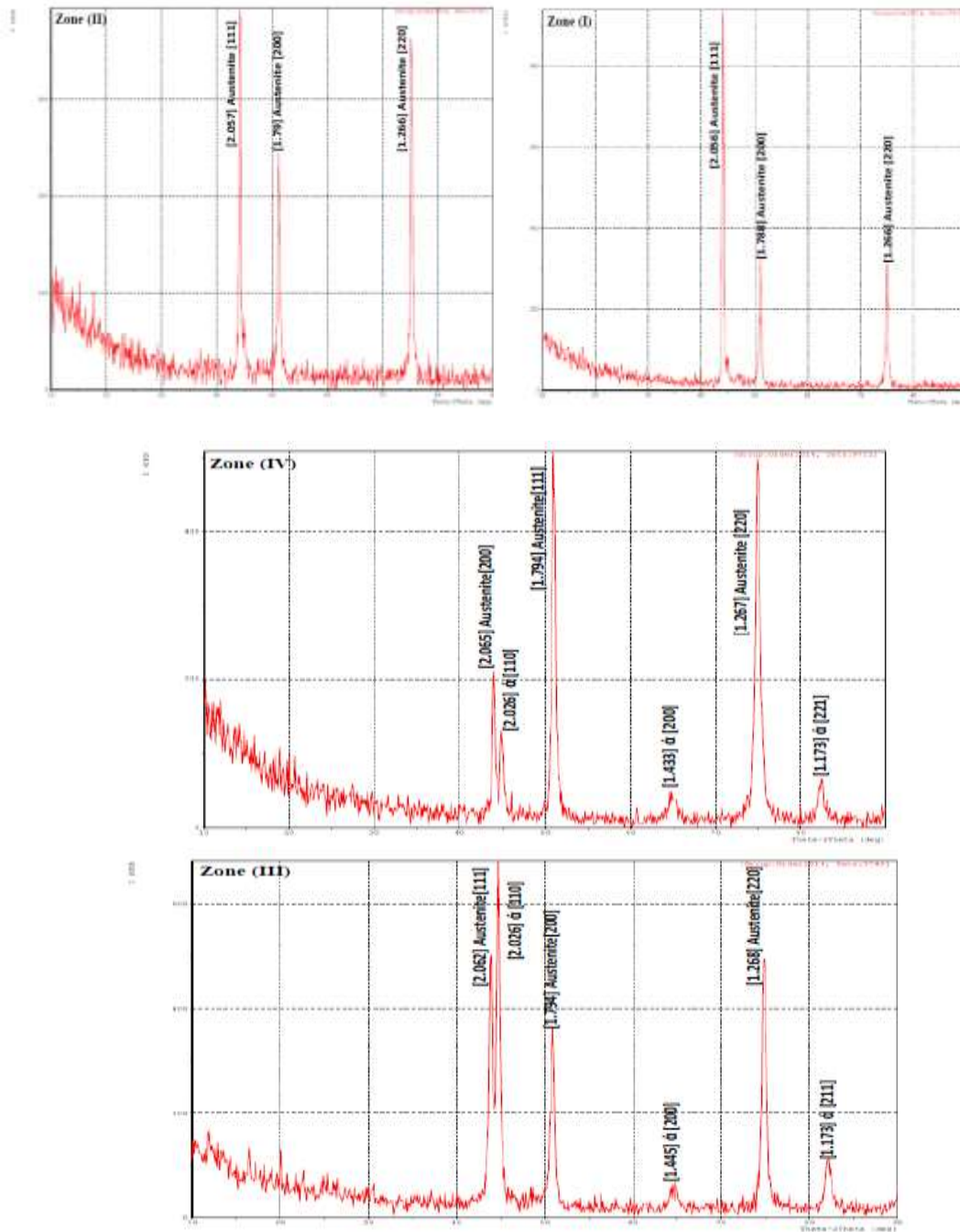
	Microstructure before corrosion	Microstructure after corrosion
<p>Zone (I) As received Hardness= 157.433 Hv</p>		
<p>Zone (II) 405MPa Hardness= (160.166 - 229.2) Hv</p>		
<p>Zone (III) 555MPa Hardness= (229.2- 332.433) Hv</p>		
<p>Zone (IV) failure Hardness= (332.433- 354.3) Hv</p>		

Figure (13) Comparison of microstructure between the different zones.



Figure( 14) X-ray diffraction spectrum[zone (I),zone(II),zone(III),zone(IV)] of 304 stainless steel.

**REFERENCES**

- [1]. W.Ozgowicz, A.Kurc, M.Kciuk, "Effect of deformation-induced martensite on the microstructure, mechanical properties and corrosion resistance of XCrNi18-8 stainless steel", international scientific journal, Vol.43,pp.42-53, 2010.
- [2]. L. Peguet, B. Malki, B. Baroux., " Influence of cold working on the pitting corrosion resistance of stainless steels", Corrosion Science, Vol. 49 ,pp. 1933–1948,2007.
- [3].L.V. Jin-long, Luo Hong-yun., " Influence of tensile pre-strain and sensitization on passive films in AISI 304 austenitic stainless steel" .,Materials Chemistry and Physics, Vol. 135 ,pp. 973-978,2012.
- [4]. S K Ghosh, P Mallick, P P Chattopadhyay, " Effect of cold deformation on phase evolution and mechanical properties in an austenitic stainless steel for structural and safety applications", journal of iron and steel research ,international.Vol .19,pp.63-68,2012.
- [5]. Jingqiang Yang, Qiongqi Wang, Kaishu Guan," Effect of stress and strain on corrosion resistance of duplex stainless steel ",International Journal of Pressure Vessels and Piping, Vol.110, pp. 72-76,2013.
- [6].D.K.Singh,"strength of materials", Second Edition, 2011.
- [7]. Vignal V, Mary N, Valot C, Oltra R, Coudreuse L."Influence of elastic deformation on initiation of pits on duplex stainless steels", Electrochemical and Solid-State Letters,Vol.7,pp.39-42,2004.
- [8]. K. Hashimoto, K. Asami, A. Kawashima, H. Habazaki and E.Akiyama," The role of corrosion-resistant alloying elements in passivity", Corrosion Science,Vol.49,pp. 42–52,2007.
- [9]. A. Kurc a, Z. Stokosa , " The effect of ( $\gamma \rightarrow \alpha'$ ) phase transformation on microstructure and properties of austenitic Cr-Ni steels" Archives of Materials Science and Engineering, Vol.38, pp. 26-33,2009.